

Solar signals in tropospheric re-analysis data: Comparing NCEP/NCAR and ERA40

H. Gleisner*, P. Thejll, M. Stendel, E. Kaas, B. Machenhauer

Danish Meteorological Institute, Lyngbyvej 100, Copenhagen, Denmark

Accepted 26 January 2005
Available online 21 April 2005

Abstract

Recent analyses of the NCEP/NCAR re-analysis data have demonstrated statistically significant variations in tropospheric temperatures, geopotential heights, water vapour distribution, and global circulation regimes in phase with the solar cycle over the last 44 years. The findings reveal a consistent pattern of atmospheric response to solar variability throughout the low- and mid-latitude troposphere. In order to more firmly establish the reality and nature of the detected Sun–climate relations, and to correctly identify the atmospheric processes involved, independent confirmation from other relevant data sets is warranted.

In this paper we present the results of identical analyses of the NCEP/NCAR and ERA40 re-analysis data sets and show that the detected Sun–climate relations are substantially weaker in the ERA40 data than in the NCEP data. We argue that this largely is due to the presence of temporal inhomogeneities in ERA40 having a substantial impact on decadal signals, which strongly affects the observed Sun–climate relations as well as climate trends. The nature of the NCEP-ERA40 differences, their influence on the detection of Sun–climate relations, and their possible causes are discussed.

© 2005 Elsevier Ltd. All rights reserved.

PACS: 96.40.Kk; 92.70.Gt

Keywords: NCEP re-analysis data; ERA40 re-analysis; Sun–climate relations; Solar cycle; Tropospheric temperature

1. Introduction

During the last decade there has been a renewed interest in the field of Sun–climate relations, largely due to observational findings that shed new light on the issue. Apparent responses to the solar cycle have been found in the stratospheric thermal and geopotential structure (Labitzke and van Loon, 1995; van Loon and Labitzke, 1993), in globally averaged lower-tropospheric temperatures (Douglass and Clader, 2002), in sea-surface

temperatures (White et al., 1997), and in the global amount of low clouds (Marsh and Svensmark, 2000; Kristjansson et al., 2002). The tropospheric response to solar variability described by these findings is generally stronger than simple radiation balance would suggest (e.g., Douglass and Clader). At the present time we cannot describe the causal chain of events leading to these observed effects, as we lack a comprehensive understanding of the atmospheric processes and possible feedbacks responding to solar variability. Even though several plausible mechanisms have been suggested, the observational findings have still not allowed us to select amongst the candidate mechanisms.

*Corresponding author.

E-mail address: hgl@dmi.dk (H. Gleisner).

The use of globally distributed sets of meteorological re-analysis data now allows us to overcome many of the limitations of past studies. Using various solar-irradiance proxies and the NCEP/NCAR re-analysis data (Kalnay et al., 1996) from the period 1958 to 2001—thus covering more than 4 solar cycles—we recently performed a comprehensive analysis of the tropospheric temperature, circulation and humidity response to solar variability on inter-annual to decadal time scales (Gleisner and Thejll, 2003) and Theiler and Prichard (1996). The effects of ENSO and volcanic emissions were removed from the atmospheric data through the use of a multi-variate regression technique, and the results demonstrated the existence of a consistent and statistically significant response to solar variability throughout the low- and mid-latitude troposphere. These results are confirmed by Haigh (2003) in an analysis of the apparent solar influences on zonal mean atmospheric temperatures obtained from the NCEP data set.

In order to more firmly establish the reality and nature of the detected Sun–climate relations, we here compare these findings based on the NCEP re-analysis data with results from an identical analysis of the ERA40 re-analysis data set produced at the European Centre for Medium Range Weather Forecasts (Simmons and Gibson, 2000). While the observational data used in the ERA40 re-analysis are largely, though not entirely, the same as that used in the NCEP re-analysis, the use of independent software and data assimilation procedures makes a comparison important, both as a means to evaluate the uncertainty of the obtained results and as a means to uncover differences between the two re-analysis data sets.

The analysis procedure here applied to both the NCEP and the ERA40 data is the same as in Gleisner and Thejll (2003). After removal of ENSO and volcanic signals from the tropospheric data, together with the effects of any forcing factors expressible as linear trends, correlations between annual means of a solar-activity proxy and climatic parameters (temperatures, geopotential heights, humidity, static stability, etc.) are mapped throughout the troposphere from the equator to the mid-latitudes. Significance levels for the correlations are estimated by a very conservative surrogate-data method. The nature of the NCEP-ERA40 differences as revealed by time series of global mean tropospheric layer thicknesses, their likely causes, and their consequences for the Sun–climate relations are then discussed.

2. Data and analysis methods

2.1. Data and pre-processing

The term “re-analysis” commonly refers to the processing of observational meteorological data by the

use of a physical model, whereby the data are made physically consistent and interpolated to a 3-D grid. In this study, we have used monthly averaged NCEP/NCAR and ERA40 re-analysis data from 1958 to 2001 (Kalnay et al., 1996; Simmons and Gibson, 2000). As a measure of solar forcing we have used the 10.7 cm solar radio flux (F_{10}), here considered as a rather general proxy for solar irradiance. Two concurrently operating forcing factors are also considered; the NINO 3 index (N3) as a proxy for forcing by the El Niño-Southern Oscillation phenomenon (ENSO) and global Atmospheric Optical Depths (AOD) (Sato et al., 1993) as a measure of volcanic forcing. A third, linear function F_{lin} represents trends of unknown origin. A time lag of 3 months is applied to N3, which is the lag that maximizes correlations between equatorial Pacific SST anomalies and global-scale atmospheric temperature anomalies (Peixoto and Oort, 1992). No delays are applied to F_{10} or AOD.

At each grid point, the monthly anomalies of all variables are computed by removing the annual cycle based on data from 1958 to 2001. The ENSO and volcanic signals are then removed from the monthly anomaly data, at each location in the grid, by the method described in Section 2.2. Any linear trends are removed as a part of this procedure. The atmospheric data from which the effects of ENSO, volcanic emissions, and any forcing factors expressible as a linear trend have been removed are henceforth termed *processed* data. As a last step, annual averages are computed from the processed monthly anomaly data, for use in the Sun–climate correlation studies described in Section 3 and in Figs. 2 and 3.

2.2. Methods

Any attempts to detect a solar signal in the atmosphere must deal with the problem of how to disentangle the effects of concurrently operating forcing factors acting on the climate, most notably ENSO, emissions from major volcanic eruptions, and solar activity. To separate the effects of these partly co-linear factors, we perform a multi-variate regression at each spatial location throughout the troposphere using N3, AOD, F_{10} , and F_{lin} as regression variables (Gleisner and Thejll, 2003):

$$O = k_0 + k_1 N3 + k_2 F_{10} + k_3 AOD + k_4 F_{lin} + \varepsilon,$$

where O is the monthly anomalies of an atmospheric observable. By subtracting the terms $k_1 N3$, $k_3 AOD$, and $k_4 F_{lin}$ from the observed data, O , we obtain the processed data, O^* , which describe all atmospheric variations that are not explained by ENSO, stratospheric aerosols, or other forcing factors primarily expressed as trends in the climate data.

We also need to address the statistical significance of the findings. To rule out chance covariations between causally unrelated time series as the cause of the detected solar signals, we have applied a very conservative surrogate-data method to estimate significance levels. Random surrogate data with similar statistical properties as the observed data—most notably similar spectral power distributions—are used to estimate the likelihoods to obtain the observed correlations by pure chance. With this method, we can effectively address problems related to the possible occurrence of decadal atmospheric variations of non-solar origin, thus minimising the risk that we erroneously accept a chance finding as support for a causal relation. See Gleisner and Thejll (2003) and Theiler and Prichard (1996) for further details about these statistical aspects.

3. Solar signals in NCEP and ERA40

Fig. 1 shows near-global averages of the upper (500–200 hPa) and lower (1000–500 hPa) tropospheric thicknesses for the NCEP (left panels) and ERA40 (right panels) data sets. The figure also shows the solar cycle as revealed by the 10.7 cm solar radio flux. Apparently, the tropospheric layer thickness has varied in phase with the solar cycle over nearly 4 cycles, particularly for NCEP but less so for ERA40. The discrepancies between

NCEP and ERA40 are particularly large in the upper troposphere. During the mid 1970s a large positive anomaly in ERA40, absent in the NCEP data, disturbs the similarity, as does the absence of a strong feature in the beginning of the 1980s. The whole period from 1973 to 1993 looks distinctly different in the two data sets, while the periods before 1973 and after 1993 look more similar.

Figs. 2 and 3 show maps of correlations between F_{10} and tropospheric layer thicknesses for both NCEP and ERA40. The corresponding 90% and 95% significance levels are shown in the maps to the right, while the plots to the left show zonal means of the correlations (thick lines) and correlations between F_{10} and zonal mean thicknesses (thin lines). The most pronounced features of the NCEP plots are that positive correlations predominate throughout the studied region, and that the solar signals show a pronounced three-banded structure. These results are more thoroughly described in Gleisner and Thejll (2003) and will not be further studied in detail here.

As expected from the large departures of the ERA40 tropospheric layer thicknesses from the solar cycle (Fig. 1), the correlation maps for ERA40 in Figs. 2 and 3 reveal substantially weaker correlations over large parts of the Earth when compared with the corresponding maps for NCEP. The upper troposphere correlation in ERA40 (Fig. 2) evidently only agrees with the NCEP patterns over

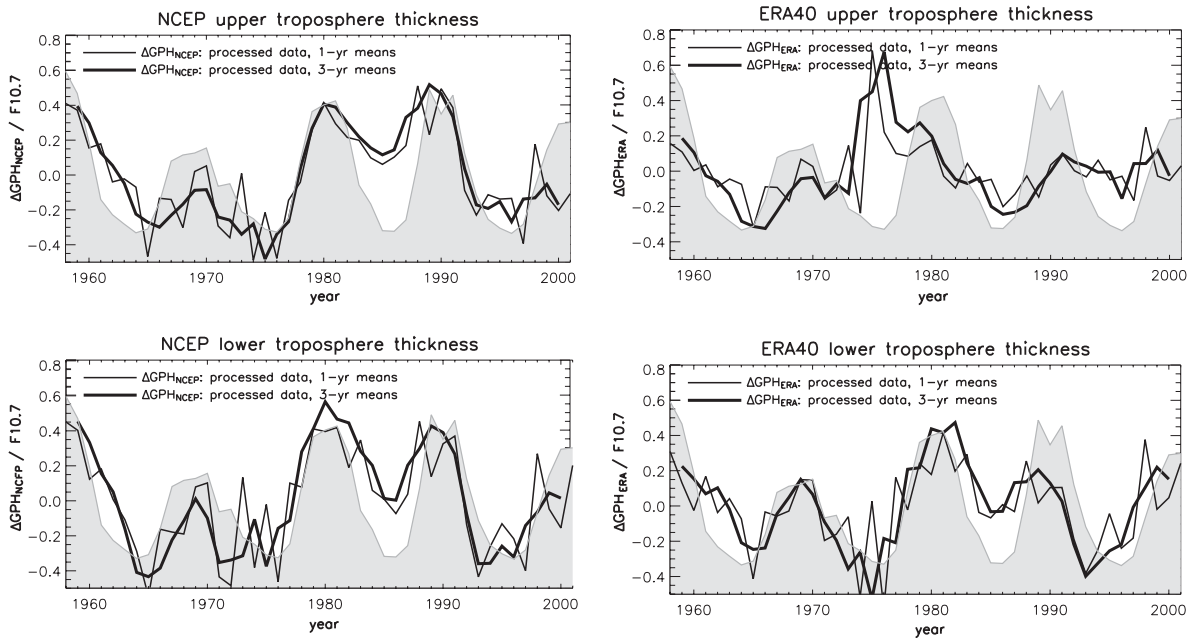


Fig. 1. Near-global averages of tropospheric thicknesses in the NCEP/NCAR (left panels) and ERA40 (right panels) re-analysis data sets. The data have been processed to remove the effects of ENSO, volcanic emissions, and linear trends. The solar activity cycle is shown for comparison, here indicated by the 10.7 cm solar radio flux (shaded). The heavy lines show 3-year sliding means while the thin lines show annual means.

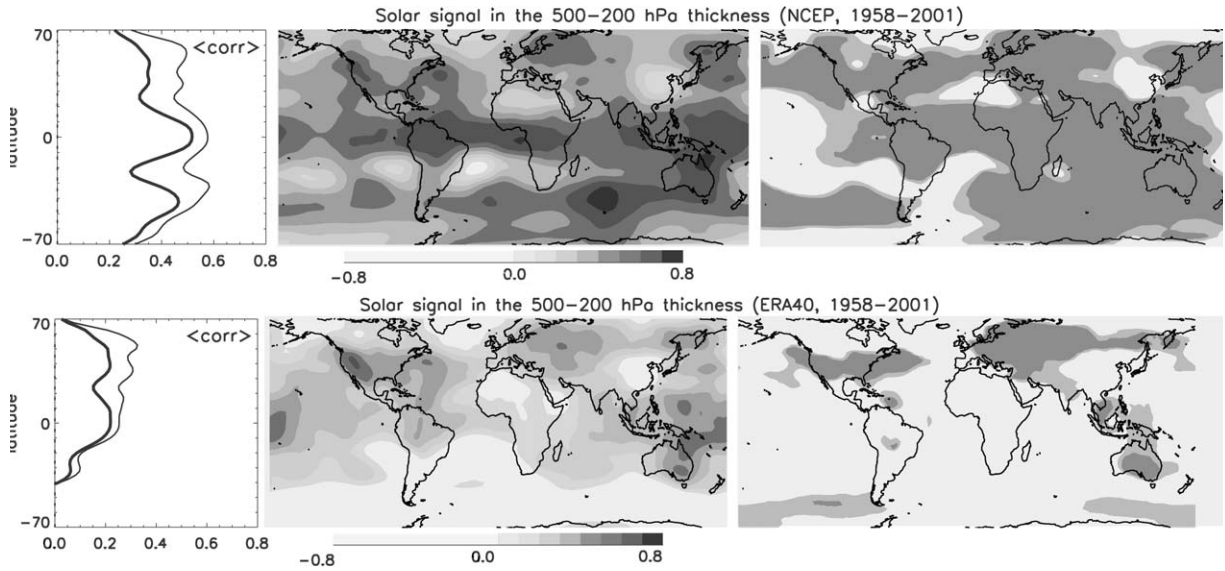


Fig. 2. Solar signals in the upper tropospheric thickness—NCEP in the upper panels and ERA40 in the lower panels. The middle panels show correlations between annual means of $F10$ and the 500–200 hPa thickness for the period 1958–2001. The panels to the left show zonal means of the correlations (thick lines) and correlations between $F10$ and zonal mean thicknesses (thin lines), while the panels to the right show the 90% (light grey) and 95% (dark grey) significance levels of the point correlations.

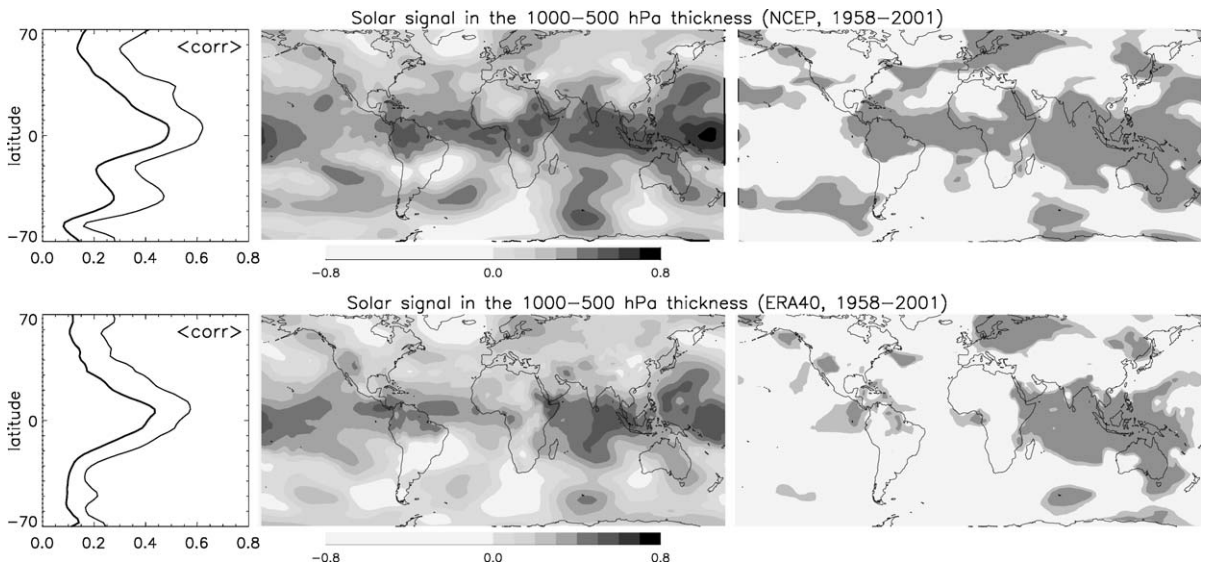


Fig. 3. Solar signals in the lower tropospheric thickness—NCEP in the upper panels and ERA40 in the lower panels. Same analysis as in Fig. 2, but for the lower troposphere.

western parts of Eurasia, Australia and the USA and western North Atlantic. In the lower troposphere (Fig. 3) agreement is better, covering the Indian Ocean to the western equatorial Pacific, northern Europe and Western Eurasia, and Australia. In general, these are regions where the re-analyses do not rely too heavily on satellites since enough conventional data (radiosonde, aircraft) are available.

4. Differences between NCEP and ERA40

Considering the strong solar signals detected in the NCEP data, and considering the fact that the NCEP and ERA40 data are arrived at through largely equivalent procedures, we would expect strong Sun–climate relations to be found also in ERA40. However, this is obviously not the case. Figs. 2 and 3 show that solar

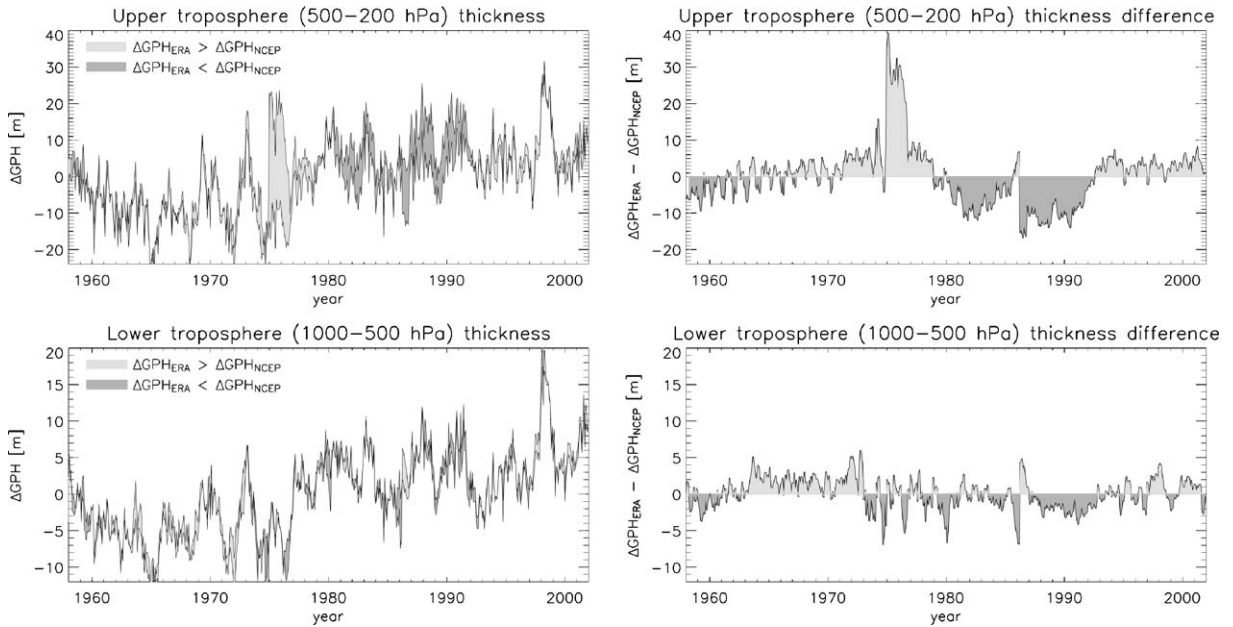


Fig. 4. Near-global averages of tropospheric layer thicknesses (left panels) obtained from the NCEP and ERA40 re-analysis data. The panels to the right show the differences between the ERA40 and NCEP time series. The plots show unprocessed anomaly data, i.e., annual cycles have been removed but the data have not been otherwise processed to remove effects due to ENSO, volcanic eruptions, or linear trends.

signals do appear in ERA40, but not as strongly and not to the same extent as in the NCEP data. The discrepancies between the two data sets that are evident in Fig. 1 offer some insights into the causes of this lack of Sun–climate correlations in ERA40. To further understand the reasons for the divergent results, we now turn to a more direct comparison of the two re-analysis data sets.

Fig. 1 shows that the temporal evolution of the climate in ERA40 is substantially different from that in NCEP. The relatively smooth decadal oscillation seen in the NCEP data is much less pronounced in ERA40, particularly in the upper troposphere and in the mid 1970s and throughout the 1980s. In Fig. 4 we now plot the monthly means of atmospheric layer thicknesses for the upper and lower troposphere. As in Fig. 1, near-global means are studied but now using unprocessed anomaly data, i.e., annual cycles have been removed but the data have not been de-trended or processed to remove the effects of ENSO or volcanic emissions. The left panels in Fig. 4 show the time series of monthly mean thicknesses, while the corresponding differences between the ERA40 and NCEP time series are shown to the right. We note that:

- the differences are larger for the upper troposphere than for the lower troposphere,
- the difference time series for the upper troposphere exhibits a trend superposed by an annual cycle from 1958 to the beginning of the 1970s,

- during the 1980s the ERA40 upper troposphere thickness was consistently lower than the corresponding NCEP thickness,
- a sudden rise in the ERA40 upper troposphere thickness in January 1975 is followed by a rapid decline in September 1976. NCEP data show no corresponding features,
- a sudden decrease of the ERA40 upper-troposphere thickness in April 1986 coincides with a sudden increase in the lower-troposphere thickness: note the anti-correlated wave-shapes in the difference time series for the two atmospheric layers. These features are found in ERA40, but not in the NCEP data.

The jump in the ERA40 upper-troposphere thickness in the mid-70’s is the most pronounced difference between the two data sets. This feature alone efficiently disrupts Sun–climate correlations due to decadal variations. It is important to note that this feature is a property of the ERA40 data only, and cannot be found in the NCEP data. The feature in the difference time series in 1986 can be traced to ERA40 as well, while the other differences do not appear to be uniquely associated with either NCEP or ERA40. In the lower troposphere, the NCEP-ERA40 differences are altogether much smaller, and appear more noise-like, except for the wave-like feature in 1986.

These results show that there are at least two major features in the NCEP-ERA40 difference time series

which are found in ERA40 but not in NCEP, and that the very same features strongly weaken the Sun–climate relations detected in ERA40. While not explaining all the differences between the solar signals derived from the two re-analysis data sets, it nevertheless appears that a large part of the differences are due to the presence of temporal inhomogeneities in ERA40 having a strong impact on decadal signals.

5. Discussion

We conclude that the different expression of the solar cycle in ERA40 and NCEP, particularly in the upper troposphere and in the period from 1973 to 1993, are due to substantial discrepancies between the two re-analysis data sets. As we have seen, some of the discrepancies have a character that would be difficult to explain solely by reference to differences amongst the observational data that enter the re-analysis procedures. The NCEP and ERA40 re-analysis data sets are currently used extensively in a wide range of studies—often by researchers not directly involved in the re-analysis work, and not fully familiar with the limitations of the data—and it appears important to identify the causes of the discrepancies.

Some of the features in the ERA40 data that strongly affect the apparent Sun–climate relations have been briefly mentioned before in the literature. Bengtsson et al. (2004) discuss trends in the ERA40 reanalysis data. The effects due to changes in observing practises are mentioned, but no direct reference to the artifacts in the mid 1970s is made. Machenhauer and Yang (2004), however, show, in considering the ERA40 total heat budget, that the sign of trends in ERA40 often are changing abruptly around 1973 and that an erroneous stratospheric heating suddenly occurred in 1975 and 1976. The temporal inhomogeneity in the ERA40 data during 1975 and 1976—which is the one single feature that most strongly decreases the Sun–climate correlations in ERA40—seems to be due to a satellite bias correction error (personal communication, Adrian Simmons, ECMWF). The feature in the difference time series in 1986, simultaneously affecting both the upper and lower troposphere, also seems to be due to inhomogeneities in the ERA40 data alone. Problems with retrievals from NOAA-6, NOAA-7 and NOAA-9, and with the bias correction when one satellite was replaced by another, have been reported for 1980 and 1986. As discussed in Stendel et al. (2000), they lead to a clear cold bias in ERA15 which translates into negative values in Fig. 4. The same feature, although weaker, is also visible in ERA40 during that period (not shown). In the lower stratosphere and upper troposphere we also see a jump in April 1986. A positive temperature bias was

introduced with NOAA-11, both in ERA15 and ERA40, which is not inconsistent with the feature visible in Fig. 4. Most of the remaining differences cannot be uniquely traced to either NCEP and ERA40.

In this study we have pointed out inhomogeneities in ERA40 which substantially weaken the observed solar signals—or indeed any decadal signals—and we have shown that no such apparent inhomogeneities are found in the NCEP data. From the current re-analysis data, we cannot unambiguously and with as much detail as we would like answer the question of how the atmosphere responds to solar variability. A better clarification of the discrepancies between the two re-analysis data sets would be helpful in this respect.

Acknowledgements

The NCEP/NCAR monthly re-analysis data were obtained from the NOAA/CDC web site, the NINO 3 index from the NOAA/CPC web site, and the solar *F*10.7 index from the NOAA/NGDC web site. The ERA40 re-analysis data were obtained from the ECMWF web site, and the AOD data were obtained from NASA's GISS web site. This work was supported by the Danish Climate Centre.

References

- Bengtsson, L., Hagemann, S., Hodges, K.I., 2004. Can climate trends be calculated from re-analysis data? MPI Report 3, ISSN 0937-1060.
- Douglass, D.H., Clader, B.D., 2002. Climate sensitivity of the Earth to solar irradiance. *Geophysical Research Letter*, doi:10.129/2002GL015345.
- Gleisner, H., Thejll, P., 2003. Patterns of tropospheric response to solar variability. *Geophysical Research Letter*, doi:10.129/2003GL017129.
- Haigh, J.D., 2003. The effects of solar variability on the Earth's climate. *Philosophical Transaction of Royal Society of London A* 361 95, 111.
- Kalnay, E., Kanamitsu, M., Kistler, R., Collins, W., Deaven, D., Gandin, L., Iredell, M., Saha, S., White, G., Woollen, J., Zhu, Y., Chelliah, M., Ebisuzaki, W., Higgins, W., Janowiak, J., Mo, K., Ropelewski, C., Wang, J., Leetmaa, A., Reynolds, R., Jenne, R., Joseph, D., 1996. The NCEP/NCAR 40-year re-analysis project. *Bulletin of the American Meteorological Society* 77, 437–471.
- Kristjánsson, J.E., Staple, A., Kristiansen, J., Kaas, E., 2002. A new look at possible connections between solar activity, clouds and climate. *Geophysical Research Letter*, doi:10.129/2002GL015646.
- Labitzke, K., van Loon, H., 1995. Connection between the troposphere and the stratosphere on a decadal scale. *Tellus A* 47, 275–286.
- van Loon, H., Labitzke, K., 1993. Review of the decadal oscillation in the stratosphere of the northern

- hemisphere. *Journal of Geophysical Research* 98, 18919–18922.
- Machenhauer, B., Yang, S., 2004. Total heat budget based on ERA40—detection of changes and their reasons, poster presented at the CLIVAR International Conference, June 21–25, Baltimore, USA.
- Marsh, N., Svensmark, H., 2000. Solar influence on Earth's climate. *Space Science Review* 107, 317–325.
- Peixoto, J.P., Oort, A.H., 1992. *Physics of Climate*. Springer, New York.
- Sato, M., Hansen, J.E., McCormick, M.P., Pollack, J.B., 1993. Stratospheric aerosol optical depth 1850–1990. *Journal of Geophysical Research* 98, 22987–22994.
- Simmons, A.J., Gibson, J.K. (Eds.), 2000. *The ECMWF Project Plan*, ECMWF Project Report Series, 1, ECMWF, Reading, UK.
- Stendel, M., Christy, J.R., Bengtsson, L., 2000. Assessing levels of uncertainty in recent temperature time series. *Climate Dynamics* 16, 587–601.
- Theiler, J., Prichard, D., 1996. Constrained-realization Monte-Carlo method for hypothesis testing. *Physica D* 94, 221–235.
- White, W.B., Lean, J., Cayan, D.R., Dettinger, M.D., 1997. Response of global upper ocean temperature to changing solar irradiance. *Journal of Geophysical Research* 102, 3255–3266.